AGU PUBLICATIONS

Geophysical Research Letters

RESEARCH LETTER
10.1002/2016GL069690

Key Points:
- Snowmelt rate drives subsurface flow and streamflow production across the western U.S.
- Western U.S. ecoregions have varying streamflow sensitivities to changes in snowmelt rate
- Earlier, slower snowmelt usually produces less streamflow than more rapid melt

Supporting Information:
- Supporting Information S1
- Supporting Information S2

Correspondence to:
T. B. Barnhart,
theodore.barnhart@colorado.edu

Citation:
Barnhart, T. B., N. P. Molotch, B. Livneh, A. A. Harpold, J. F. Knowles, and D. Schneider (2016), Snowmelt rate dictates streamflow, *Geophys. Res. Lett.*, *43*, 8006–8016, doi:10.1002/2016GL069690.

Received 23 MAY 2016
Accepted 2 JUL 2016
Accepted article online 6 JUL 2016
Published online 3 AUG 2016

Snowmelt rate dictates streamflow

Theodore B. Barnhart[1,2], Noah P. Molotch[1,2,3], Ben Livneh[4,5], Adrian A. Harpold[6], John F. Knowles[2], and Dominik Schneider[1,2]

[1]Department of Geography, University of Colorado Boulder, Boulder, Colorado, USA, [2]Institute of Arctic and Alpine Research, University of Colorado Boulder, Boulder, Colorado, USA, [3]Jet Propulsion Laboratory, California Institute of Technology, Pasadena, California, USA, [4]Department of Civil, Environmental, and Architectural Engineering, University of Colorado Boulder, Boulder, Colorado, USA, [5]Cooperative Institute for Research in Environmental Sciences, University of Colorado Boulder, Boulder, Colorado, USA, [6]Department of Natural Resources and Environmental Science, University of Nevada, Reno, Reno, Nevada, USA

Abstract Declining mountain snowpack and earlier snowmelt across the western United States has implications for downstream communities. We present a possible mechanism linking snowmelt rate and streamflow generation using a gridded implementation of the Budyko framework. We computed an ensemble of Budyko streamflow anomalies (BSAs) using Variable Infiltration Capacity model-simulated evapotranspiration, potential evapotranspiration, and estimated precipitation at 1/16° resolution from 1950 to 2013. BSA was correlated with simulated baseflow efficiency ($r^2 = 0.64$) and simulated snowmelt rate ($r^2 = 0.42$). The strong correlation between snowmelt rate and baseflow efficiency ($r^2 = 0.73$) links these relationships and supports a possible streamflow generation mechanism wherein greater snowmelt rates increase subsurface flow. Rapid snowmelt may thus bring the soil to field capacity, facilitating below-root zone percolation, streamflow, and a positive BSA. Previous works have shown that future increases in regional air temperature may lead to earlier, slower snowmelt and hence decreased streamflow production via the mechanism proposed by this work.

1. Introduction

Mountain snowpack and snowmelt-derived streamflow are a critical water resource for approximately one sixth of the global population [*Barnett et al*., 2005]. However, trends in observed peak snow water equivalent (SWE) and the timing of spring snowmelt indicate that the western United States (U.S.) mountain snowpack is declining and that snowmelt onset is occurring earlier in the year [*Clow*, 2010; *Harpold et al*., 2012]. Correspondingly, trends in streamflow records show that snowmelt-driven streamflow is also occurring earlier in the year both in the western U.S. and globally [*Cayan*, 1996; *Stewart et al*., 2004, 2005; *Stewart*, 2009]. These trends suggest that snowpack accumulation and melt dynamics are responding to higher near-surface air temperatures and changes in precipitation magnitude and phase driven by regional climate change [*Knowles et al*., 2006; *Luce et al*., 2014]. As climate change violates the critical stationarity assumption for statistical water supply forecast models [*Milly et al*., 2008], a process-based understanding of the snowmelt-streamflow relationship, and how this relationship varies regionally, is needed to better predict water availability.

In addition to changing precipitation type, climate warming also shifts the timing of snowmelt earlier in spring [*Hamlet et al*., 2005]. Previous work suggests that earlier snowmelt may alter streamflow production through two opposing mechanisms: (i) Earlier snowmelt, due to a warmer atmosphere, partitions a greater proportion of snowmelt to evapotranspiration (ET) than streamflow because of atmospheric warming-induced increased vapor pressure deficit [e.g., *Bosson et al*., 2012]. Conversely, (ii) early snowmelt disrupts the synchrony between water availability and vegetation water demand and results in greater streamflow because water delivery occurs when vegetation is less active [*Jeton et al*., 1996]. Recent results by *Trujillo and Molotch* [2014], which showed that earlier snowmelt is associated with slower snowmelt, lead us to a third hypothesis (iii) in which slower snowmelt decreases streamflow generation. This hypothesis is rooted in the soil water balance whereby snowmelt rates in excess of evapotranspiration rates may increase infiltration in excess of field capacity, leading to greater subsurface drainage. In this way, snowmelt rate may control the relative hydrological partitioning of snowmelt between ET and streamflow production. Rapid snowmelt may thus drive subsurface flow below the root zone and/or result in melt rates that exceed infiltration rates, leading to overland flow; both mechanisms could generate high Budyko streamflow anomalies (BSAs) and

lead to proportionally greater streamflow. Furthermore, hypothesis iii is consistent with previous work highlighting the coupling between snowmelt timing and peak soil moisture [*Harpold and Molotch*, 2015] and the distribution and magnitude of soil water for facilitating subsurface flow from variable snowmelt rates [*Wilcox et al*., 1997; *Liu et al*., 2004; *McNamara et al*., 2005; *Flint et al*., 2008; *Liu et al*., 2008; *Jencso et al*., 2009; *Graham et al*., 2010; *Chauvin et al*., 2011; *Liu et al*., 2012; *Harpold and Molotch*, 2015].

In this study, we test the validity of hypothesis iii and propose a potential mechanism to explain this behavior. We do not attempt to test hypotheses i or ii in this study. We specifically investigate the relationship between snowmelt rate and streamflow production by testing (a) to what degree snowmelt rate explains Budyko-based streamflow production (BSA), (b) whether there exists a clear mechanism linking snowmelt rate to streamflow production, and (c) if regional heterogeneity in the snowmelt rate-streamflow production relationship is present across the western U.S.

2. Data and Domain

To compare the relationship between snowmelt rate and Budyko-based streamflow production, we used a gridded hydrometeorological data set [*Livneh et al*., 2015] containing consistent daily meteorological forcings and simulated Variable Infiltration Capacity (VIC) model states and fluxes at 1/16° (~6 km) resolution from 1950 to 2013 [*Liang et al*., 1994]. Daily forcing and simulated variables included station-derived precipitation (P), minimum and maximum air temperature, simulated evapotranspiration (ET_{VIC}), potential evapotranspiration (PET), streamflow (Q), baseflow (Q_{bf}), and SWE. Daily values of PET in VIC are calculated using the Penman-Monteith equation [*Shuttleworth*, 1993]. Baseflow is defined in VIC as water that passes through the soil column and is thus analogous to shallow subsurface flow. Runoff in VIC is defined as water that travels over the land surface and in the near-surface soil. Discharge (Q) is the sum of runoff and baseflow.

The VIC model has previously been applied to simulate the mountain snowpack in many studies [*Hamlet and Lettenmaier*, 1999; *Hamlet and Huppert*, 2002; *Mote et al*., 2005; *Elsner et al*., 2010; *Vano and Lettenmaier*, 2012; *Vano et al*., 2015], and the snow model within VIC has been validated against observations [*Andreadis et al*., 2009] and compared against other land surface models [*Feng et al*., 2008; *Chen et al*., 2014]. A full iterative energy balance option was selected for VIC, while an explicit frozen soil option was not selected, to ensure a conservative estimate of spring runoff magnitude and rate, acknowledging that overestimating frozen soil effects could overstate linkages between snowmelt and streamflow. Frozen soils are also rare in snow-covered, mountainous locations because the snow acts to insulate the ground from below freezing air temperatures. The *Livneh et al*. [2015] data set used for this study utilized the same VIC version number and parameterization as *Livneh et al*. [2013], which was validated against streamflow observations for the major river basins of the conterminous U.S. We conduct our own VIC validation in section 3.4.

We masked the *Livneh et al*. [2015] data set to our domain of interest, which was a composite of the major mountainous Level III ecoregions [*CEC*, 2011] of the western U.S. (Figure 1) and contained 19,983 simulation grid cells. The specific ecoregions included the Cascades, Eastern Cascades Slopes and Foothills, North Cascades, Sierra Nevada, Wasatch and Uinta Mountains, Idaho Batholith, Northern Rockies, Canadian Rockies, Southern Rockies, and Middle Rockies. We selected this domain because all these regions have appreciable snow accumulation and generate runoff for downstream communities [*Bales et al*., 2006]. Unless otherwise stated, analyses are reported for the entire domain as a whole.

3. Methods

To test hypothesis iii, we evaluated the correlation between VIC-modeled snowmelt rate and VIC-modeled BSA values for all grid cells within the domain (Figure 1). We then masked the domain into its component ecoregions and evaluated the interregional sensitivity of streamflow production to snowmelt rate. This represents an evaluation of streamflow production anomalies (Figure S1a in the supporting information) that is analogous to the approach of *Berghuijs et al*. [2014] who used the *Budyko* [1974] relationship, which relates long-term ET/P to long-term PET/P. However, several works have argued that the use of universal Budyko-type functional relationships may not be appropriate over different climatic regions [*Choudhury*, 1999; *Zhang et al*., 2001; *Zhou et al*., 2015]. Hence, for our ecoregion-specific analysis, we also fit *Zhang et al*. [2001] Budyko-type equations for each ecoregion and extracted the y axis asymptote from these fitted

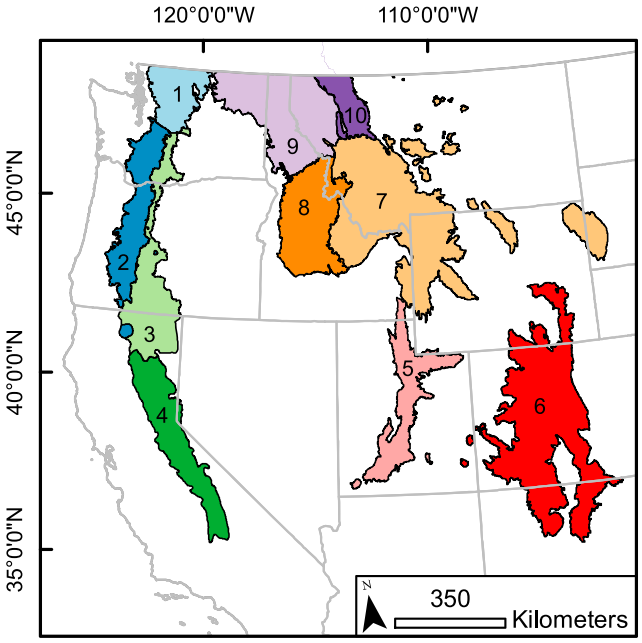

Figure 1. The simulation domain covers the mountainous ecoregions of the western United States. Included ecoregions are (1) North Cascades, (2) Cascades, (3) Eastern Cascades Slopes and Foothills, (4) Sierra Nevada, (5) Wasatch and Uinta Mountains, (6) Southern Rockies, (7) Middle Rockies, (8) Idaho Batholith, (9) Northern Rockies, and (10) Canadian Rockies.

Budyko-type relationships as a metric of the minimum hydrologic partitioning of precipitation to streamflow for each ecoregion (Figure S1b). Additionally, we examined the regional variation in the BSA-snowmelt rate relationship. This approach allowed us to test the influence of snowmelt rate on Budyko streamflow production across the entire domain as well as within specific regions, using both the fitted Budyko-type equation and an ensemble of Budyko equations.

3.1. Snowmelt Rate

We calculated the long-term average snowmelt rate (Sm_j) as

$$Sm_j = \frac{\sum \Delta SWE_{j,t}}{D_j} \quad (1)$$

where j is the grid cell, t is the simulation day (summed from 1 January 1950 to 31 December 2013), $\Delta SWE_{j,t} = SWE_{j,t} - SWE_{j,t-1}$, and D_j is the number of days where $\Delta SWE_{j,t} < 0$. Positive $\Delta SWE_{j,t}$ values represent accumulation events and were forced to zero when calculating Sm_j. During the melt season we assumed that latent heat fluxes would be preferentially partitioned to melt rather than sublimation when the snowpack was isothermal [*Hood et al.*, 1999] due to the order-of-magnitude difference between the latent heats of fusion and sublimation of water (334 kJ kg^{-1} and 2834 kJ kg^{-1}, respectively). We also assumed negligible wind redistribution of snow across 1/16° grid cells [*Tabler*, 2003].

3.2. The Budyko Framework

Budyko [1974] provides a framework to compare streamflow and evaporative partitioning of different watersheds for a given amount of available energy and precipitation. This is accomplished by plotting a basin's long-term average aridity index (PET/*P*) on the horizontal axis versus the long-term evaporative index (ET/*P*) on the vertical axis (Figure S1a). We used an ensemble of the nine Budyko-type equations from Table 1 in *Zhou et al.* [2015], four of which incorporate fitting parameters [*Mezentsev*, 1955; *Fu*, 1981; *Choudhury*, 1999; *Zhang et al.*, 2001, 2004; *Yang et al.*, 2008; *Zhou et al.*, 2015] and five of which do not [*Schreiber*, 1904; *Ol'Dekop*, 1911; *Turc*, 1955; *Pike*, 1964; *Budyko*, 1974; *Sharif et al.*, 2007]. This type of analysis has been applied in numerous studies as an organizational framework within which to compare catchments [e.g., *Wagener et al.*, 2007; *Berghuijs et al.*, 2014; *Troch et al.*, 2015], to look at streamflow production across catchments [e.g., *Donohue et al.*, 2011], and to assess catchment-scale energy versus moisture limitation [e.g., *Jones et al.*, 2012; *Creed et al.*, 2014; *Knowles et al.*, 2015].

Accordingly, we used each Budyko-type equation from *Zhou et al.* [2015] to derive a theoretical ET/*P*, which we then compared to VIC-modeled ET/*P* in order to determine if a given grid cell was more or less efficient at generating streamflow than predicted by the Budyko-type equation. To relate ET/*P* to streamflow efficiency (*Q*/*P*), we used the long-term water balance for each grid cell, which assumes no long-term changes in storage:

$$Q = P - \mathrm{ET} \quad (2)$$

and *Q*/*P* is specifically related to ET/*P* by

$$\frac{Q}{P} = 1 - \frac{\mathrm{ET}}{P} \quad (3)$$

Similar to *Berghuijs et al*. [2014], we calculated the Budyko-predicted streamflow efficiency (Q_{Budyko}/P) for each grid cell using the long-term, simulated PET/*P* of each grid cell by substituting the Budyko-type equation into equation (3) such that

$$\frac{Q_{Budyko}}{P} = 1 - f\left(\frac{PET}{P}\right) \tag{4}$$

where *f*(PET/*P*) is one of the nine Budyko-type equations from *Zhou et al*. [2015]. Therefore, a grid cell with an evaporative index approaching unity partitions very little water to streamflow, while a grid cell with an evaporative index approaching zero partitions most water to streamflow. Simulated streamflow efficiency (Q_{VIC}/P) was computed as

$$\frac{Q_{VIC}}{P} = 1 - \frac{ET_{VIC}}{P} \tag{5}$$

Finally, we computed BSA (i.e., a streamflow production metric) for each grid cell as

$$BSA = \frac{Q_{anom}}{P} = \frac{Q_{VIC}}{P} - \frac{Q_{Buydko}}{P} \tag{6}$$

Grid cells that plotted below the Budyko-type curve (Figure S1a) had positive BSA values (equation (6)), indicating that these grid cells produced more streamflow than expected from the Budyko-type equation. Conversely, grid cells that plotted above the curve (Figure S1a) had negative BSA values, indicating that these grid cells produced less streamflow than expected from the Budyko-type equation. For example, if a location with a positive BSA transitioned to a negative BSA, then this would represent a reduction in streamflow efficiency, which could have important implications for water availability at that location.

This approach yielded an ensemble of nine BSA estimates. For clarity, we present the mean BSA for each grid cell and the mean statistical relationships between mean BSA and snowmelt rate, baseflow efficiency (Q_{bf}/P), and snowfall fraction as determined by linear regression. We present statistics for each BSA and independent variable combination in the supporting information.

3.3. Regional Analysis

For our regional analysis, we evaluated the correlation of VIC-derived snowmelt rate and the BSA ensemble for each ecoregion. Similar to section 3.2, we present mean relationships and report statistics for all relationships in the supporting information. In addition, we correlated the evaporative index asymptote of the *Zhang et al*. [2001] Budyko-type curve, a metric of the minimum hydrologic partitioning to streamflow for each ecoregion (Figure S1b), with mean ecoregion snowmelt rate. These two comparisons are complementary and represent two different ways of using the Budyko framework to evaluate hydrologic controls on streamflow generation. To derive asymptotes for each ecoregion, we fit the *Zhang et al*. [2001] Budyko-type equation for each ecoregion. We then extracted the fitted Budyko-type equation evaporative index (*y* axis) asymptote (Figure S1b). We also calculated the mean snowmelt rate for each ecoregion by taking the mean of the Sm_j values for all VIC grid cells within each ecoregion.

3.4. Model Validation

The *Livneh et al*. [2015] data set was validated against observational streamflow and three gridded precipitation data sets: Daymet [*Thornton et al*., 1997], Maurer [*Maurer et al*., 2002], and the North American Land Data Assimilation System [*Xia et al*., 2012] for 671 catchments [*Newman et al*., 2015]. Three precipitation data sets were used given the inherent uncertainty in precipitation estimates over mountainous terrain. We then computed the long-term streamflow coefficient (*Q*/*P*) for each catchment using VIC-simulated *Q* and *P* estimated from *Livneh et al*. [2015] cropped to the extent of each catchment. These VIC-derived streamflow coefficients were then compared to streamflow coefficients generated using the observed streamflow and the three gridded precipitation data sets. The resulting VIC-simulated streamflow coefficients compared favorably against the streamflow coefficients derived using the observational data sets provided in *Newman et al*. [2015] with regression slopes ranging from 0.83 to 0.96 (p values < 0.001, r^2 values > 0.93, Figure S2). This demonstrates that the long-term average precipitation partitioning between ET and *Q* of the *Livneh et al*. [2015] data set was reasonable.

4. Results

4.1. Snowmelt Rate and Hydrologic Partitioning

In general, the VIC-simulated aridity and evaporative indices followed the mean Budyko curve (Figure 2a). However, a substantial portion of the domain fell below the curve, especially grid cells with low aridity indices; statistics for each Budyko-type equation are presented in Table S1. The average ensemble mean BSA ± one standard deviation for the entire domain was 0.04 ± 0.1 (statistically different from zero, *t* test $p < 0.001$), indicating that the domain slightly overproduced streamflow for a given amount of precipitation and available energy relative to the mean Budyko curve. The domain included grid cells that both underproduced and overproduced streamflow with 5th and 95th percentile mean BSA values of 0.04 and 0.20, respectively (Figure 2b). This indicates that while the mean was relatively close to zero, there was significant variability in streamflow production with 5% of the domain underproducing streamflow and 5% of the domain overproducing streamflow by 20% or more relative to the mean Budyko curve (Figure 2b).

The mean snowmelt rate across the domain was 4.4 ± 3.2 mm d^{-1}, and the 5th and 95th percentile snowmelt rates were 1.0 and 10.7 mm d^{-1}, respectively. Snowmelt rate significantly explained the variance in mean BSA ($r^2 = 0.42$, $p < 0.001$, Figure 2b), which demonstrates that grid cells with more rapid snowmelt often produced more streamflow than expected from the mean Budyko curve. Statistical data for the BSA-snowmelt rate relationship, for each Budyko-type equation, are given in Table S2. We note that snowmelt rate was a poor predictor of mean BSA at snowmelt rates below 2.5 mm d^{-1} and that mean BSA was distinctly positive at snowmelt rates above 12.5 mm d^{-1} (Figure 2b).

A more complex linear regression for the mean BSA-snowmelt rate relationship ($y = 0.01x + 0.06\ln(x) - 0.07$; Figure 2b) yielded a slightly better fit (r^2 of 0.47 compared to 0.42), but we chose to use the simple linear regression for further analysis because the slope of this linear regression is easily interpreted as a metric of the sensitivity of mean BSA to a change in snowmelt rate. Differences in the sensitivity of mean BSA to a change in snowmelt rate between ecoregions are presented in section 4.2.

We also found a strong relationship between snowmelt rate and VIC-derived baseflow efficiency ($r^2 = 0.73$, $p < 0.001$, Figure 2c), linking snowmelt rate to subsurface flow production in VIC. Additionally, we found a linear relationship between baseflow efficiency and mean BSA ($r^2 = 0.64$, $p < 0.001$, Figure 2d). Together, these relationships suggest that rapid snowmelt results in greater baseflow efficiency, which ultimately produces higher BSA values (Figures 2b–2d). Statistics for the BSA-baseflow efficiency relationship for each Budyko-type equation are given in Table S3.

4.2. Regional Sensitivity to Changes in Snowmelt Rate

The slope of the mean BSA-snowmelt relationship for each ecoregion shows the sensitivity of streamflow production in each ecoregion to a unit change in snowmelt rate (Figure 3a). Slopes for each ecoregion ranged from 0.047 in the Northern Rockies to 0.007 in the Southern Rockies. Although all relationships in Figure 3a were significant with $p < 0.001$, the amount of variance explained by each relationship varied from 74% to 9% for the Cascades and Northern Rockies, respectively. In total, 8 of 10 ecoregion snowmelt rate-mean BSA relationships had $r^2 > 0.3$. Statistical data for each snowmelt-BSA relationship and ecoregion are reported in Table S4.

Fitted *Zhang et al*. [2001] Budyko-type equations for each ecoregion exhibited a wide range of curve asymptotes, whereby minimum partitioning to streamflow varied from 3% to 30% of precipitation (i.e., asymptotes ranged from 0.97 to 0.70; Figure 3b and Table S5). The mean ecoregion snowmelt rate values for the minimum and maximum asymptotes are 2.47 and 8.18 mm d^{-1}, respectively (Table S5). The variability in fitted *Zhang et al*. [2001] asymptotes is well explained by mean ecoregion snowmelt rate ($r^2 = 0.87$, $p < 0.001$, Figure 3c).

5. Discussion

5.1. Snowmelt Rate Controls Hydrologic Partitioning

We note that especially in more rain-dominated locations, field capacity may be reached in autumn prior to the development of a snowpack thereby complicating the proposed mechanism. The snowmelt rate-excess soil water mechanism described above is also invalid when the snowmelt rate is greater than the infiltration

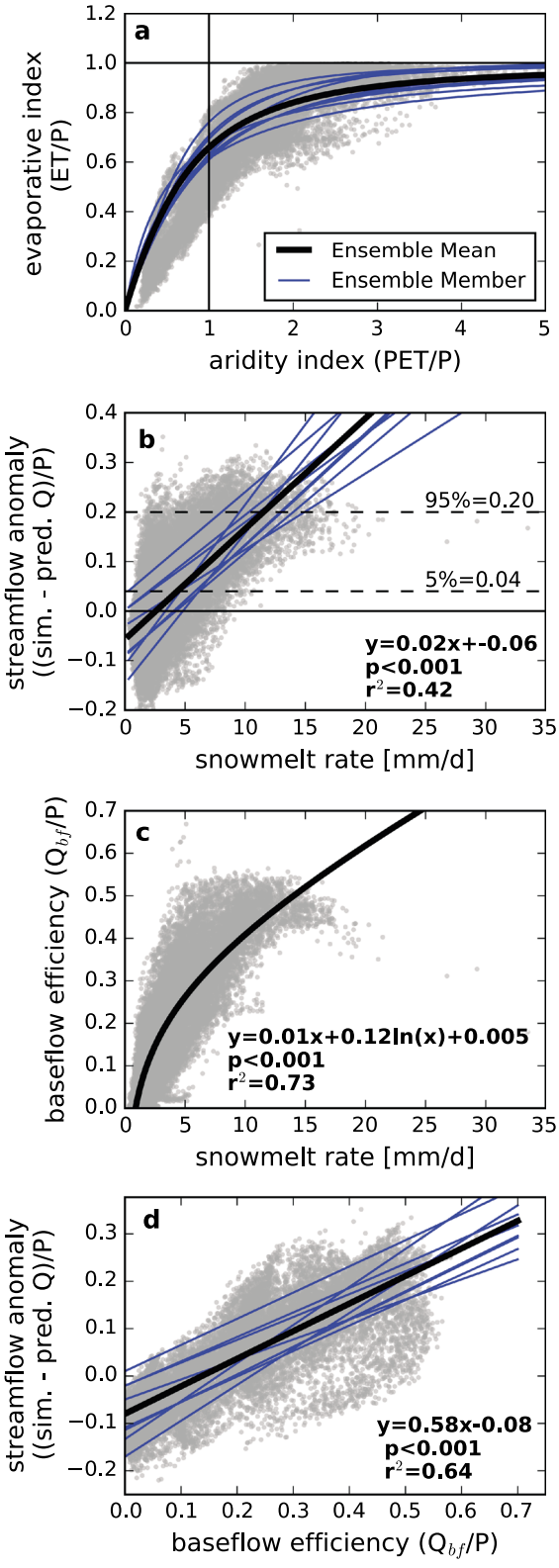

Figure 2. (a) Simulation grid cells (grey dots) plotted in Budyko space and the mean Budyko curve (black line). The ensemble of Budyko-type equations is shown as blue lines. (b) Relationship between snowmelt rate and mean BSA (black line). The same relationship for each Budyko-type equation is shown using blue lines. (c) Relationship between snowmelt rate and baseflow efficiency (Q_{bf}/P). (d) Relationship between baseflow efficiency and mean BSA (black line). The same relationship for each Budyko-type equation is shown using blue lines.

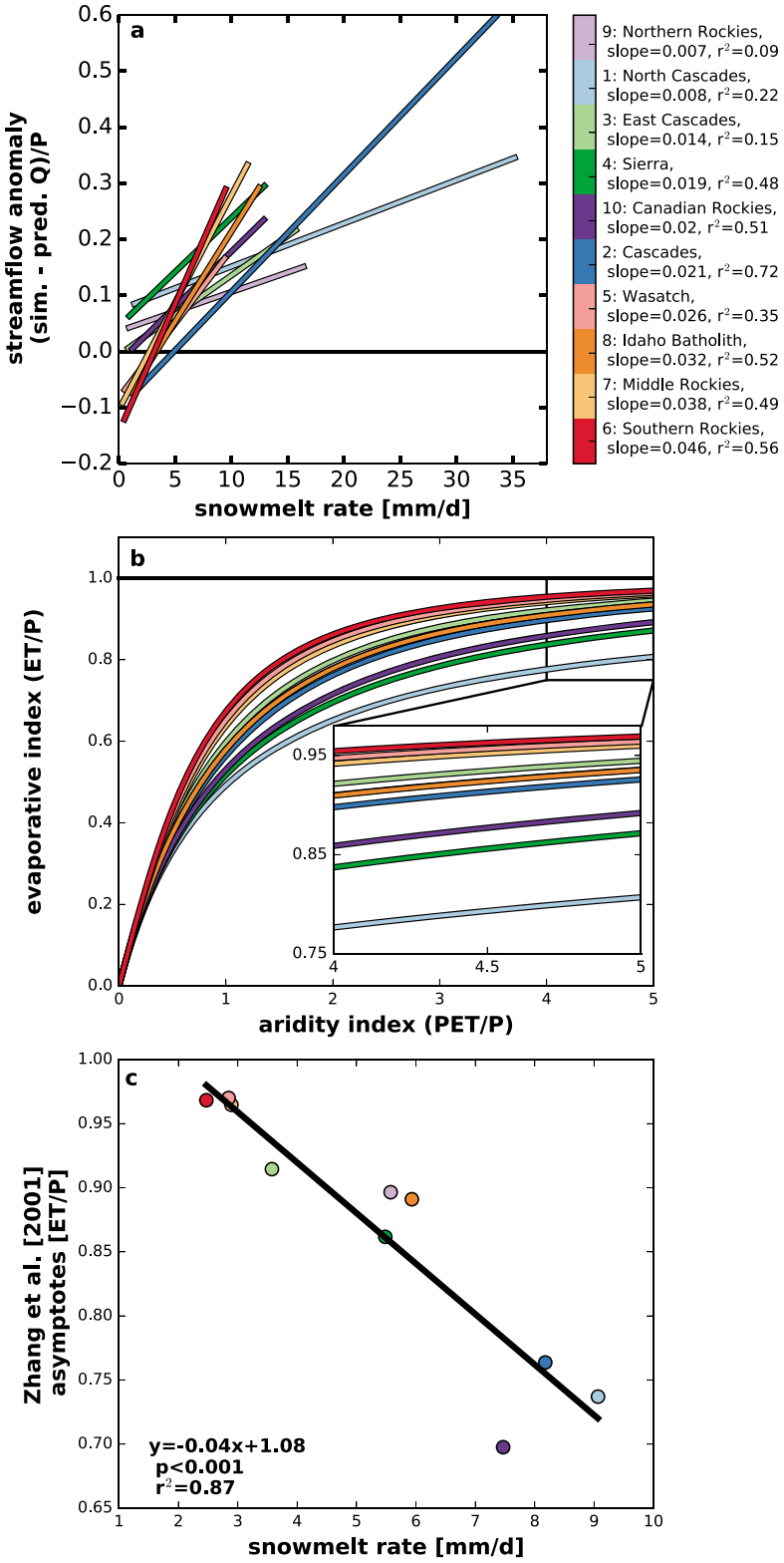

Figure 3. (a) Regressions between snowmelt rate and mean BSA for each ecoregion. Index numbers for each ecoregion (right) are the same as in Figure 1. All regressions are significant ($p < 0.001$). Regression lines extend to the range of the data. (b) *Zhang et al.* [2001] Buydko-type equations fitted to each ecoregion with inset highlighting variability in the asymptotes. (c) Relationship between ecoregion asymptotes and mean ecoregion snowmelt rate. All panels use the same color scheme.

capacity of the soil, although this scenario is unlikely in the absence of bedrock or frozen soil [*Wilcox et al*., 1997]. The strong relationship between baseflow efficiency and mean BSA suggests that infiltration excess overland flow, i.e., runoff in VIC, is not driving high BSA values.

The analysis presented here shows that rapid snowmelt promotes greater streamflow anomalies by driving greater baseflow, which is consistent with previous snowmelt-driven streamflow analyses. Previous studies have identified lateral subsurface flow as a major contributor to streamflow in snowmelt-dominated catchments using direct measurements [*Wilcox et al*., 1997; *McNamara et al*., 2005; *Graham et al*., 2010; *Chauvin et al*., 2011]. Other studies have used hydrograph separation to infer the contribution of lateral subsurface flow to streamflow [*Liu et al*., 2004, 2008, 2012]. In line with our potential mechanism of streamflow anomaly generation, *Flint et al*. [2008] showed that rapid snowmelt rates greater than 1.6 cm d^{-1} are capable of exceeding bedrock permeability and inducing lateral subsurface flow in the Sierra Nevada, California. Given the consistency with previous work, the snowmelt-streamflow mechanism presented here may represent a broadly applicable theory for snowmelt-driven streamflow production across the western U.S. wherein snowmelt in excess of evapotranspiration brings the soil column to field capacity and drives subsurface flow.

This work demonstrates that across the western U.S., areas with more rapid snowmelt overproduced streamflow relative to Budyko-type model expectations (Figure 2b). We showed that grid cells with rapid snowmelt also have high baseflow efficiency, which strongly correlated with mean BSA (Figures 2b–2d). This pattern fits with our hypothesis (iii) wherein rapid snowmelt is linked to high BSA values. This pattern also suggests a potential snowmelt rate-driven streamflow generation mechanism, whereby rapid snowmelt delivers water to the soil column, bringing it above field capacity, inducing percolation below the root zone, and contributing to excess soil water. Excess soil water then leads to increased subsurface flow, which results in elevated BSA values. In contrast, when this relationship is inverted, slower snowmelt corresponds to lower, even negative, BSA values, suggesting a decrease in proportional streamflow production and greater partitioning to evapotranspiration.

Snowmelt has been shown to play an important role in low summer streamflow [*Godsey et al*., 2014]. Projections of climate warming for snow-dominated locations suggest that summertime streamflow will decrease by about 30% due to earlier snowmelt and the subsequent drawdown of shallow groundwater [*Huntington and Niswonger*, 2012]. Our study establishes a novel mechanistic link between snowmelt rate, excess soil water, and BSA to reinforce the importance of snowmelt for streamflow production via the subsurface.

Work comparing snowmelt rates observed at snowpack telemetry sites across the western U.S. showed that earlier melt occurred at a slower melt rate because there was less solar radiation to drive snowmelt earlier in the year [*Trujillo and Molotch*, 2014]. Additionally, *Trujillo and Molotch* [2014] found that within ecoregions of the western U.S., sites that experienced greater SWE accumulations tended to peak later in the year and that these sites also experience later, more rapid snowmelt. Due to these interrelationships, snowmelt rate thus represents an integrating metric of snowpack amount and melt timing. Furthermore, for a given soil type, runoff production due to rainfall versus snowfall inputs is dictated by the balance between the rate of water delivery—i.e., rainfall and snowmelt—and the rate of evaporative losses to the atmosphere. Our analyses, when combined with previously identified negative trends in mountain snowpack and melt rates, suggest that earlier, slower snowmelt may reduce percolation below the root zone resulting in proportionally less streamflow.

5.2. Regional Sensitivity to Changes in Snowmelt Rate

The relationship between the *Zhang et al*. [2001] asymptotes and the mean ecoregion snowmelt rates (Figure 3c) suggests that minimum hydrologic partitioning to streamflow is controlled by snowmelt rate. This corroborates the idea that snowmelt rate controls streamflow production via a secondary analysis. When individual ecoregion BSA-snowmelt relationships were examined for the entire study domain (Figure 3a), all of the regression slopes were positive and 89 of 90 relationships had slopes significantly different from zero ($p < 0.05$), indicating that decreased snowmelt rate led to an overall decrease in BSA throughout the domain.

A wide range of sensitivities of mean BSA to changes in snowmelt rate were observed across the domain (section 4.2 and Figure 3a). The significant range of explained variance by the mean BSA-snowmelt relationship

for each ecoregion (9–72%) also suggests that the BSA-snowmelt relationship may be dominant in some regions, while streamflow production in other locations may be due to other mechanisms. Additionally, the observed range of sensitivities and explained variance (Figure 3a) may be due to variable meteorological controls on snowmelt rate and streamflow production, e.g., rain during the snowmelt season and throughout the snow-free portions of the year. Alternatively, these ranges could also be the result of differences in soil properties and depth [*Flint et al*., 2008], elevation, and/or vegetation as represented by the parameterization of the *Livneh et al*. [2015] data set.

The combination of the asymptote-snowmelt relationship (Figures 3b and 3c) and ecoregion-specific mean BSA-snowmelt relationships (Figure 3a) shows an interesting pattern in snowmelt rate and streamflow production across the western U.S. Namely, ecoregions that had higher BSA sensitivities to snowmelt rate in Figure 3a also had lower average snowmelt rates and high asymptotes in Figure 3c. This may be because these ecoregions were more continental with generally shallower snowpacks that melted more slowly than maritime regions with deeper snowpacks and more rapid mean snowmelt rates [*Trujillo and Molotch*, 2014]. For example, the same change in snowmelt rate for a site that generally experienced slow snowmelt (e.g., the Southern Rockies) was proportionally larger than for a site that generally experienced rapid snowmelt (e.g., the North Cascades), and the subsequent effect on streamflow production was then proportionally larger for the slow snowmelt region than for the rapid snowmelt region.

5.3. Snowmelt Rate and Snowfall Fraction

Berghuijs et al. [2014] attributed differences in BSA values to differences in snowfall fraction ($r^2 = 0.303$, $p < 0.001$) across 420 Model Parameter Estimation Experiment (MOPEX) catchments. We also found a positive correlation between snowfall fraction (as computed in Text S1) and mean BSA ($r^2 = 0.3$, $p < 0.001$, Figure S3 and Table S6). Earlier work, however, demonstrated that sites with greater snowfall fractions tend to have greater peak SWE [*Serreze et al*., 1999] and that these sites melt later and more rapidly than sites with less peak SWE [*Trujillo and Molotch*, 2014]. We thus propose that the relationship between snowfall fraction and BSA, found by *Berghuijs et al*. [2014], may be due to the collinearity between snowfall fraction and snowmelt rate ($r^2 = 0.31$, $p < 0.001$, Figure S4). This relationship was robust with rain-snow temperature thresholds for equation (S2) ranging from −2 to 2°C ($p < 0.001$, $r^2 = 0.20$ and 0.40, respectively). In this context, snowmelt rate, as shown here, provides an explanatory mechanism for future analyses of streamflow sensitivity to snowmelt dynamics. Conversely, snowfall fraction, itself, is not a streamflow-generating metric. Furthermore, the data used for this study include landscapes with significantly greater snowfall fractions than those within the MOPEX data set used by *Berghuijs et al*. [2014] and, therefore, may provide a more comprehensive analysis.

6. Conclusion

Shifts toward earlier, slower snowmelt from regional warming have broad hydrologic implications in the western United States and globally. This work represents a unique, grid-cell-by-grid-cell, application of the Budyko framework to the western United States, which is accompanied by a detailed regional intercomparison using fitted Budyko-type equations. We tested the hypothesis that snowmelt rate controls Budyko streamflow anomaly and thus hydrologic partitioning of snowmelt between evapotranspiration and streamflow production. The results suggested that (1) snowmelt rate was strongly correlated with mean Budyko streamflow anomaly across the western United States ($r^2 = 0.42$, $p < 0.001$), (2) locations with high snowmelt rates had greater baseflow efficiency ($r^2 = 0.73$, $p < 0.001$), (3) locations with high baseflow efficiency corresponded to greater mean Budyko streamflow anomalies ($r^2 = 0.64$, $p < 0.001$), and that (4) the variance in minimum ecoregion streamflow production (i.e., *Zhang et al*. [2001] asymptotes) was well explained by mean ecoregion snowmelt rate ($r^2 = 0.87$, $p < 0.001$). These results imply that hydrologic partitioning across the western United States may be broadly controlled by snowmelt rate and that snowmelt rate-driven soil water excess may be responsible for both observed and modeled positive Budyko streamflow anomalies. At smaller scales, western United States ecoregions exhibited a wide range of mean Budyko streamflow anomaly-snowmelt rate sensitivities highlighting the potential modulating influence of meteorology and soil properties. This study provides a means to relate future changes in snowpack to streamflow dynamics across the western United States and elsewhere, toward the goal of constraining the expected streamflow response to climate change. Future efforts should concentrate on correctly predicting changes in snowmelt rate from warming as well as understanding the regional differences in the Budyko streamflow anomaly-snowmelt rate relationship.

Acknowledgments

We would like to thank Paul Brooks for his comments on an early version of this work, M. Bayani Cardenas for his suggestion to include an ensemble of Budyko-type equations, and Jeff Dozier for his comments on the manuscript. This work was supported by the USDA-NSF Water Sustainability and Climate grant (2012-67003-19802), NSF Boulder Creek CZO (EAR-9810218), NSF Hydrological Sciences (EAR-1141764), NSF (EAR-1144894), USDA NIFA (NEV05293), NSF Niwot Ridge LTER (DEB-1027341), and a NASA Earth and Space Science Fellowship to D.S. This analysis was conducted in iPython 2.7 (https://ipython.org/) using Jupyter (http://jupyter.org/), Pandas (http://pandas.pydata.org/), Numpy (http://www.numpy.org/), Matplotlib (http://matplotlib.org/), and Statsmodels (http://statsmodels.sourceforge.net/devel/). Data used for this analysis are available at ftp://192.12.137.7/pub/dcp/archive/OBS/livneh2014.1_16deg/ and are cited in section 2.

References

Andreadis, K. M., P. Storck, and D. P. Lettenmaier (2009), Modeling snow accumulation and ablation processes in forested environments, *Water Resour. Res.*, *45*, W05429, doi:10.1029/2008WR007042.

Bales, R., N. P. Molotch, T. H. Painter, M. D. Dettinger, R. Rice, and J. Dozier (2006), Mountain hydrology of the western United States, *Water Resour. Res.*, *42*, W08432, doi:10.1029/2005WR004387.

Barnett, T. P., J. C. Adam, and D. P. Lettenmaier (2005), Potential impacts of a warming climate on water availability in snow-dominated regions, *Nature*, *438*(7066), 303–309, doi:10.1038/nature04141.

Berghuijs, W. R., R. A. Woods, and M. Hrachowitz (2014), A precipitation shift from snow towards rain leads to a decrease in streamflow, *Nat. Clim. Change*, *4*(7), 583–586, doi:10.1038/nclimate2246.

Bosson, E., U. Sabel, L.-G. Gustafsson, M. Sassner, and G. Destouni (2012), Influences of shifts in climate, landscape, and permafrost on terrestrial hydrology, *J. Geophys. Res.*, *117*, D05120, doi:10.1029/2011JD016429.

Budyko, M. I. (1974), *Climate and Life*, Academic Press, New York.

Cayan, D. R. (1996), Interannual climate variability and snowpack in the western United States, *J. Clim.*, *9*(5), 928–948, doi:10.1175/1520-0442(1996)009<0928:ICVASI>2.0.CO;2.

CEC (2011), *North American Terrestrial Ecoregions—Level III*, Comm. for Environ. Cooperation, Montreal, Canada.

Chauvin, G. M., G. N. Flerchinger, T. E. Link, D. Marks, A. H. Winstral, and M. S. Seyfried (2011), Long-term water balance and conceptual model of a semi-arid mountainous catchment, *J. Hydrol.*, *400*(1–2), 133–143, doi:10.1016/j.jhydrol.2011.01.031.

Chen, F., et al. (2014), Modeling seasonal snowpack evolution in the complex terrain and forested Colorado Headwaters region: A model intercomparison study, *J. Geophys. Res. Atmos.*, *119*, 13,795–13,819, doi:10.1002/(ISSN)2169-8996.

Choudhury, B. J. (1999), Evaluation of an empirical equation for annual evaporation using field observations and results from a biophysical model, *J. Hydrol.*, *216*(1-2), 99–110, doi:10.1016/S0022-1694(98)00293-5.

Clow, D. W. (2010), Changes in the timing of snowmelt and streamflow in Colorado: A response to recent warming, *J. Clim.*, *23*(9), 2293–2306, doi:10.1175/2009JCLI2951.1.

Creed, I. F., et al. (2014), Changing forest water yields in response to climate warming: Results from long-term experimental watershed sites across North America, *Global Change Biol.*, *20*(10), 3191–3208, doi:10.1111/gcb.12615.

Donohue, R. J., M. L. Roderick, and T. R. McVicar (2011), Assessing the differences in sensitivities of runoff to changes in climatic conditions across a large basin, *J. Hydrol.*, *406*(3–4), 234–244, doi:10.1016/j.jhydrol.2011.07.003.

Elsner, M. M., L. Cuo, N. Voisin, J. S. Deems, A. F. Hamlet, J. A. Vano, K. E. B. Mickelson, S.-Y. Lee, and D. P. Lettenmaier (2010), Implications of 21st century climate change for the hydrology of Washington State, *Clim. Change*, *102*(1–2), 225–260, doi:10.1007/s10584-010-9855-0.

Feng, X., A. Sahoo, K. Arsenault, P. Houser, Y. Luo, and T. J. Troy (2008), The impact of snow model complexity at three CLPX sites, *J. Hydrometeor*, *9*(6), 1464–1481, doi:10.1175/2008JHM860.1.

Flint, A. L., L. E. Flint, and M. D. Dettinger (2008), Modeling soil moisture processes and recharge under a melting snowpack, *Vadose Zone J.*, *7*(1), 350–359, doi:10.2136/vzj2006.0135.

Fu, B. P. (1981), On the calculation of the evaporation from land surface [in Chinese], *Sci. Atmos. Sin.*, *5*(1), 23–31.

Godsey, S. E., J. W. Kirchner, and C. L. Tague (2014), Effects of changes in winter snowpacks on summer low flows: Case studies in the Sierra Nevada, California, USA, *Hydrol. Process.*, *28*(19), 5048–5064, doi:10.1002/hyp.9943.

Graham, C. B., W. van Verseveld, H. R. Barnard, and J. J. McDonnell (2010), Estimating the deep seepage component of the hillslope and catchment water balance within a measurement uncertainty framework, *Hydrol. Process.*, *24*(25), 3631–3647, doi:10.1002/hyp.7788.

Hamlet, A., and D. Lettenmaier (1999), Columbia River streamflow forecasting based on ENSO and PDO climate signals, *J. Water Resour. Plann. Manage.*, *125*(6), 333–341, doi:10.1061/(ASCE)0733-9496(1999)125:6(333).

Hamlet, A. F., and D. Huppert (2002), Economic value of long-lead streamflow forecasts for Columbia River hydropower, *J. Water Resour. Plann. Manage.*, *128*(2), 91–101, doi:10.1061/(ASCE)0733-9496(2002)128:2(91).

Hamlet, A. F., P. W. Mote, M. P. Clark, and D. P. Lettenmaier (2005), Effects of temperature and precipitation variability on snowpack trends in the Western United States, *J. Clim.*, *18*(21), 4545–4561, doi:10.1175/JCLI3538.1.

Harpold, A. A., and N. P. Molotch (2015), Sensitivity of soil water availability to changing snowmelt timing in the western U.S., *Geophys. Res. Lett.*, *42*, 8011–8020, doi:10.1002/2015GL065855.

Harpold, A., P. Brooks, S. Rajagopal, I. Heidbuchel, A. Jardine, and C. Stielstra (2012), Changes in snowpack accumulation and ablation in the intermountain west, *Water Resour. Res.*, *48*, W11501, doi:10.1029/2012WR011949.

Hood, E., M. Williams, and D. Cline (1999), Sublimation from a seasonal snowpack at a continental, mid-latitude alpine site, *Hydrol. Process.*, *13*(12–13), 1781–1797, doi:10.1002/(SICI)1099-1085(199909)13:12/13<1781::AID-HYP860>3.0.CO;2-C.

Huntington, J. L., and R. G. Niswonger (2012), Role of surface-water and groundwater interactions on projected summertime streamflow in snow dominated regions: An integrated modeling approach, *Water Resour. Res.*, *48*, W11524, doi:10.1029/2012WR012319.

Jencso, K. G., B. L. McGlynn, M. N. Gooseff, S. M. Wondzell, K. E. Bencala, and L. A. Marshall (2009), Hydrologic connectivity between landscapes and streams: Transferring reach- and plot-scale understanding to the catchment scale, *Water Resour. Res.*, *45*, W04428, doi:10.1029/2008WR007225.

Jeton, A. E., M. D. Dettinger, and J. Smith (1996), *Potential Effects of Climate Change on Streamflow, Eastern and Western Slopes of the Sierra Nevada, California and Nevada*, U.S. Geol. Surv., Sacramento, Calif.

Jones, J. A., et al. (2012), Ecosystem processes and human influences regulate streamflow response to climate change at long-term ecological research sites, *BioScience*, *62*(4), 390–404, doi:10.1525/bio.2012.62.4.10.

Knowles, J. F., A. A. Harpold, R. Cowie, M. Zeliff, H. R. Barnard, S. P. Burns, P. D. Blanken, J. F. Morse, and M. W. Williams (2015), The relative contributions of alpine and subalpine ecosystems to the water balance of a mountainous, headwater catchment, *Hydrol. Process.*, *29*(22), 4794–4808, doi:10.1002/hyp.10526.

Knowles, N., M. D. Dettinger, and D. R. Cayan (2006), Trends in snowfall versus rainfall in the Western United States, *J. Clim.*, *19*(18), 4545–4559, doi:10.1175/JCLI3850.1.

Liang, X., D. P. Lettenmaier, E. F. Wood, and S. J. Burges (1994), A simple hydrologically based model of land surface water and energy fluxes for general circulation models, *J. Geophys. Res.*, *99*, 14,415–14,428, doi:10.1029/94JD00483.

Liu, F., M. W. Williams, and N. Caine (2004), Source waters and flow paths in an alpine catchment, Colorado Front Range, United States, *Water Resour. Res.*, *40*, W09401, doi:10.1029/2004WR003076.

Liu, F., R. Bales, M. H. Conklin, and M. E. Conrad (2008), Streamflow generation from snowmelt in semi-arid, seasonally snow-covered, forested catchments, Valles Caldera, New Mexico, *Water Resour. Res.*, *44*, W12443, doi:10.1029/2007WR006728.

Liu, F., C. Hunsaker, and R. Bales (2012), Controls of streamflow generation in small catchments across the snow-rain transition in the Southern Sierra Nevada, California, *Hydrol. Process.*, *27*(14), 1959–1972, doi:10.1002/hyp.9304.
Livneh, B., E. A. Rosenberg, C. Lin, and B. Nijssen (2013), A long-term hydrologically based dataset of land surface fluxes and states for the conterminous United States: Update and extensions, *J. Clim.*, *26*, 9384–9392, doi:10.1175/JCLI-D-12-00508.s1.
Livneh, B., T. J. Bohn, D. W. Pierce, F. Munoz-Arriola, B. Nijssen, R. Vose, D. R. Cayan, and L. Brekke (2015), A spatially comprehensive, hydrometeorological data set for Mexico, the U.S., and Southern Canada 1950–2013, *Sci. Data*, *2*, 150042, doi:10.1038/sdata.2015.42.
Luce, C. H., V. Lopez-Burgos, and Z. Holden (2014), Sensitivity of snowpack storage to precipitation and temperature using spatial and temporal analog models, *Water Resour. Res.*, *50*, 9447–9462, doi:10.1002/2013WR014844.
Maurer, E. P., A. W. Wood, J. C. Adam, D. P. Lettenmaier, and B. Nijssen (2002), A long-term hydrologically based dataset of land surface fluxes and states for the conterminous United States, *J. Clim.*, *15*(22), 3237–3251, doi:10.1175/1520-0442(2002)015<3237:ALTHBD>2.0.CO;2.
McNamara, J. P., D. Chandler, M. Seyfried, and S. Achet (2005), Soil moisture states, lateral flow, and streamflow generation in a semi-arid, snowmelt-driven catchment, *Hydrol. Process.*, *19*(20), 4023–4038, doi:10.1002/hyp.5869.
Mezentsev, V. S. (1955), More on the calculation of average total evaporation, *Meteorol. Gidrol.*, *5*, 24–26.
Milly, P. C. D., J. Betancourt, M. Falkenmark, R. M. Hirsch, Z. W. Kundzewicz, D. P. Lettenmaier, and R. J. Stouffer (2008), Stationarity is dead: Whither water management?, *Science*, *319*(5863), 573–574, doi:10.1126/science.1151915.
Mote, P. W., A. F. Hamlet, M. P. Clark, and D. P. Lettenmaier (2005), Declining mountain snowpack in western North America, *Bull. Am. Meteorol. Soc.*, *86*(1), 39–49, doi:10.1175/BAMS-86-1-39.
Newman, A. J., et al. (2015), Development of a large-sample watershed-scale hydrometeorological data set for the contiguous USA: Data set characteristics and assessment of regional variability in hydrologic model performance, *Hydrol. Earth Syst. Sci.*, *19*(1), 209–223, doi:10.5194/hess-19-209-2015.
Ol'Dekop, E. M. (1911), On the evaporation from the surface of river basins, *Trans. Meteorol. Obs. Univ. Tartu*, *4*, 200.
Pike, J. G. (1964), The estimation of annual run-off from meteorological data in a tropical climate, *J. Hydrol.*, *2*(2), 116–123, doi:10.1016/0022-1694(64)90022-8.
Schreiber, P. (1904), Über die Beziehungen zwischen dem Niederschlag und der Wasserfürung der Flüsse, *Z. Meteorol.*, *21*, 441–452.
Serreze, M. C., M. P. Clark, R. L. Armstrong, D. A. McGinnis, and R. S. Pulwarty (1999), Characteristics of the western United States snowpack from snowpack telemetry (SNOTEL) data, *Water Resour. Res.*, *35*(7), 2145–2160, doi:10.1093/ejo/21.3.311.
Sharif, H. O., W. T. Crow, N. L. Miller, and E. F. Wood (2007), Multidecadal high-resolution hydrologic modeling of the Arkansas/Red River Basin, *J. Hydrometeor.*, *8*(5), 1111–1127, doi:10.1175/JHM622.1.
Shuttleworth, W. J. (1993), Evaporation, in *Handbook of Hydrology*, edited by D. R. Maidment, pp. 4.1–4.53, McGraw-Hill Education, New York.
Stewart, I. T. (2009), Changes in snowpack and snowmelt runoff for key mountain regions, *Hydrol. Process.*, *23*(1), 78–94, doi:10.1002/hyp.7128.
Stewart, I. T., D. R. Cayan, and M. D. Dettinger (2004), Changes in snowmelt runoff timing in western North America under a "business as usual" climate change scenario, *Clim. Change*, *62*(1–3), 217–232, doi:10.1023/B:CLIM.0000013702.22656.e8.
Stewart, I. T., D. R. Cayan, and M. D. Dettinger (2005), Changes toward earlier streamflow timing across western North America, *J. Clim.*, *18*(8), 1136–1155, doi:10.1175/JCLI3321.1.
Tabler, R. D. (2003), Controlling blowing and drifting snow with snow fences and road design, National Cooperative Highway Research Program Project 20-7(147), Transportation Research Board of the National Academies.
Thornton, P. E., S. W. Running, and M. A. White (1997), Generating surfaces of daily meteorological variables over large regions of complex terrain, *J. Hydrol.*, *190*(3–4), 214–251, doi:10.1016/S0022-1694(96)03128-9.
Troch, P. A., T. Lahmers, A. Meira, R. Mukherjee, J. W. Pedersen, T. Roy, and R. Valdés-Pineda (2015), Catchment coevolution: A useful framework for improving predictions of hydrological change?, *Water Resour. Res.*, *51*(7), 4903–4922, doi:10.1002/2015WR017032.
Trujillo, E., and N. P. Molotch (2014), Snowpack regimes of the Western United States, *Water Resour. Res.*, *50*(7), 5611–5623, doi:10.1002/2013WR014753.
Turc, L. (1955), Le bilan d"eau des sols. Relations entre le précipitations, l"évapotranspiration potentielle, *Ann. Agron. Serie A*, *5*, 491–595.
Vano, J. A., and D. P. Lettenmaier (2012), Hydrologic sensitivities of Colorado River runoff to changes in precipitation and temperature, *J. Hydrometeor.*, *13*(3), 932–949, doi:10.1175/JHM-D-11-069.1.
Vano, J. A., B. Nijssen, and D. P. Lettenmaier (2015), Seasonal hydrologic responses to climate change in the Pacific Northwest, *Water Resour. Res.*, *51*, 1959–1976, doi:10.1002/2014WR015909.
Wagener, T., M. Sivapalan, P. Troch, and R. Woods (2007), Catchment classification and hydrologic similarity, *Geogr. Compass*, *1*(4), 901–931, doi:10.1111/j.1749-8198.2007.00039.x.
Wilcox, B. P., B. D. Newman, D. Brandes, D. W. Davenport, and K. Reid (1997), Runoff from a semiarid Ponderosa pine hillslope in New Mexico, *Water Resour. Res.*, *33*(10), 2301–2314, doi:10.1029/97WR01691.
Xia, Y., et al. (2012), Continental-scale water and energy flux analysis and validation for the North American Land Data Assimilation System project phase 2 (NLDAS-2): 1. Intercomparison and application of model products, *J. Geophys. Res.*, *117*, D03109, doi:10.1029/2011JD016048.
Yang, H., D. Yang, Z. Lei, and F. Sun (2008), New analytical derivation of the mean annual water-energy balance equation, *Water Resour. Res.*, *44*, W03410, doi:10.1029/2007WR006135.
Zhang, L., W. R. Dawes, and G. R. Walker (2001), Response of mean annual evapotranspiration to vegetation changes at catchment scale, *Water Resour. Res.*, *37*(3), 701–708, doi:10.1029/2000WR900325.
Zhang, L., K. Hickel, W. R. Dawes, F. H. S. Chiew, A. W. Western, and P. R. Briggs (2004), A rational function approach for estimating mean annual evapotranspiration, *Water Resour. Res.*, *40*, W02502, doi:10.1029/2003WR002710.
Zhou, S., B. Yu, Y. Huang, and G. Wang (2015), The complementary relationship and generation of the Budyko functions, *Geophys. Res. Lett.*, *42*, 1781–1790, doi:10.1002/2015GL063511.